**Article details**

GLIA
WILEY

**RESEARCH ARTICLE**

# Localization of the cannabinoid type-1 receptor in subcellular astrocyte compartments of mutant mouse hippocampus

Ana Gutiérrez-Rodríguez[1,2] | Itziar Bonilla-Del Río[1,2] | Nagore Puente[1,2] |
Sonia M. Gómez-Urquijo[1,2] | Christine J. Fontaine[7] | Jon Egaña-Huguet[1,2] |
Izaskun Elezgarai[1,2] | Sabine Ruehle[3] | Beat Lutz[3] | Laurie M. Robin[4,5] |
Edgar Soria-Gómez[1,2] | Luigi Bellocchio[4,5] | Jalindar D. Padwal[6] |
Mario van der Stelt[6] | Juan Mendizabal-Zubiaga[1,2] | Leire Reguero[1,2] |
Almudena Ramos[1,2] | Inmaculada Gerrikagoitia[1,2] | Giovanni Marsicano[4,5] |
Pedro Grandes[1,2,7]

[1]Department of Neurosciences, University of the Basque Country UPV/EHU, Leioa, E-48940, Spain

[2]Achucarro Basque Center for Neuroscience, Science Park of the UPV/EHU, Leioa, Spain

[3]Institute of Physiological Chemistry and German Resilience Center, University Medical Center of the Johannes Gutenberg University Mainz, Mainz, 55128, Germany

[4]INSERM, U1215 Neurocentre Magendie, Endocannabinoids and Neuroadaptation, Bordeaux, F-33077, France

[5]Université de Bordeaux, Bordeaux, F-33077, France

[6]Department of Molecular Physiology, Leiden University, Einsteinweg 55, Leiden, CC, 2333, The Netherlands

[7]Division of Medical Sciences, University of Victoria, Victoria, British Columbia, V8P 5C2, Canada

**Correspondence**
Pedro Grandes, Department of Neurosciences, University of the Basque Country UPV/EHU, Barrio Sarriena s/n, E-48940 Leioa, Spain.
Email: pedro.grandes@ehu.eus

**Funding information**
The Basque Government, Grant Number: BCG IT764-13; MINECO/FEDER, UE, Grant Number: SAF2015-65034-R; University of the Basque Country, Grant Number: UPV/EHU UFI11/41; Instituto de Salud Carlos III (ISCIII), European Union-European Regional Development Fund (EU-ERDF), Subprograma RETICS Red de Trastornos Adictivos, Grant Number: RD16/0017/0012; INSERM; EU–FP7, Grant Number: PAINCAGE, HEALTH-603191; European Research Council, Grant Number: Endofood, ERC–2010–StG–260515; Fondation pour la Recherche Medicale, Grant Number: DRM20101220445; Human Frontier Science Program; Region Aquitaine; Agence Nationale de la Recherche, Grant Number: ANR Blanc ANR-13-BSV4–0006-02; German Research Foundation, Grant Number: DFG CRC/TRR 58; Vanier Canada Graduate Scholarship (NSERC)

## Abstract

Astroglial type-1 cannabinoid ($CB_1$) receptors are involved in synaptic transmission, plasticity and behavior by interfering with the so-called tripartite synapse formed by pre- and post-synaptic neuronal elements and surrounding astrocyte processes. However, little is known concerning the subcellular distribution of astroglial $CB_1$ receptors. In particular, brain $CB_1$ receptors are mostly localized at cells′ plasmalemma, but recent evidence indicates their functional presence in mitochondrial membranes. Whether $CB_1$ receptors are present in astroglial mitochondria has remained unknown. To investigate this issue, we included conditional knock-out mice lacking astroglial $CB_1$ receptor expression specifically in glial fibrillary acidic protein (GFAP)-containing astrocytes (GFAP-$CB_1$-KO mice) and also generated genetic rescue mice to re-express $CB_1$ receptors exclusively in astrocytes (GFAP-$CB_1$-RS). To better identify astroglial structures by immunoelectron microscopy, global $CB_1$ knock-out ($CB_1$-KO) mice and wild-type ($CB_1$-WT) littermates were intra-hippocampally injected with an adeno-associated virus expressing humanized renilla green fluorescent protein (hrGFP) under the control of human GFAP promoter to generate GFAPhrGFP-$CB_1$-KO and -WT mice, respectively. Furthermore, double immunogold (for $CB_1$) and immunoperoxidase (for GFAP or hrGFP) revealed that $CB_1$ receptors are present in astroglial mitochondria from different hippocampal regions of $CB_1$-WT, GFAP-$CB_1$-RS and GFAPhrGFP-$CB_1$-WT mice. Only non-specific gold particles were detected in mouse hippocampi lacking $CB_1$ receptors. Altogether, we demonstrated the existence of a precise molecular architecture of the $CB_1$ receptor in astrocytes that will have to be taken into account in evaluating the functional activity of cannabinergic signaling at the tripartite synapse.

# 1 | INTRODUCTION

Glial cells constitute the most abundant cell population in the central nervous system. The astrocytes at the tripartite synapse establish bidirectional communication with neurons by both intricate morphological non-overlapping domains (Halassa, Fellin, Takano, Dong, & Haydon, 2007) and biochemical and signaling interactions (Araque et al., 2014; Bezzi & Volterra, 2011) that play important roles in brain metabolic processes (Magistretti & Allaman, 2015), in the maintenance and regulation of synaptic physiology (Araque et al., 2014; Perez-Alvarez, Navarrete, Covelo, Martin, & Araque, 2014) and in brain information processing (Volterra & Meldolesi, 2005).

The endocannabinoid (eCB) system is composed of the seven-transmembrane G protein coupled cannabinoid type-1 ($CB_1$) receptor and other receptors (including $CB_2$ receptors), their endogenous lipid ligands (endocannabinoids) and the proteins involved in synthesis, transport and degradation of the endocannabinoids (Katona & Freund, 2012; Lutz, Marsicano, Maldonado, & Hillard, 2015; Pertwee, 2015; Piomelli, 2003). This system is widely distributed in the central and peripheral nervous system (Katona & Freund, 2012; Lu & Mackie, 2016), and also in peripheral organs (Piazza, Cota, & Marsicano, 2017), where the $CB_1$ receptors are also localized in mitochondria of striated and heart muscles (Mendizabal-Zubiaga et al., 2016). The eCB system regulates brain functions by acting on different cell types and cellular compartments (Busquets-Garcia, Bains, & Marsicano, 2018; Gutiérrez-Rodríguez et al., 2017; Katona & Freund, 2012; Lu & Mackie, 2016). The activation of $CB_1$ receptors in astrocytes promotes astroglial differentiation (Aguado et al., 2006) and mediates neuron-astrocyte communication that plays a role in synaptic plasticity, memory and behavior (Araque et al., 2014; Gómez-Gonzalo et al., 2015; Han et al., 2012; Metna-Laurent & Marsicano, 2015; Navarrete & Araque, 2008, 2010; Navarrete, Diez, & Araque, 2014; Oliveira da Cruz, Robin, Drago, Marsicano, & Metna-Laurent, 2015). Furthermore, $CB_1$ receptor activation is involved in energy supply to the brain through the control of leptin receptor expression in astrocytes (Bosier et al., 2013).

The $CB_1$ receptor-mediated astrocyte functions are highly dependent on the $CB_1$ receptor distribution in astrocytes relative to close neuronal compartments, particularly at synapses (Bonilla-Del Río et al., 2017). However, the low $CB_1$ receptor expression in astrocytes (Bosier et al., 2013; Han et al., 2012; Kovács et al., 2017; Rodriguez, Mackie, & Pickel, 2001) and mitochondria (Bénard et al., 2012; Hebert-Chatelain et al., 2014a; b; 2016) constrains a consolidated picture of the subcellular $CB_1$ receptor distribution in the astroglial compartments that holds the anatomical substrate for a functional interaction with the nearby synapses under normal or pathological conditions (Bonilla-Del Río et al., 2017). Yet, whether intracellular $CB_1$ receptors exist in astroglial mitochondria has remained unknown. In the hippocampus, mitochondrial

$CB_1$ ($mtCB_1$) receptor activation affects synaptic transmission and memory formation through reduced phosphorylation of specific subunits of the complex I electron transport system, and through decreased mitochondrial respiration and mobility (Hebert-Chatelain et al., 2016). These effects are due to intra-mitochondrial $G\alpha i$ protein activation by $mtCB_1$ receptors that leads to the inhibition of soluble adenylyl cyclase and, consequently, to the decrease in intra-mitochondrial protein kinase A (PKA) activity (Hebert-Chatelain et al., 2016). New tools based on genetic rescue strategies have proven to be useful to dissect the sufficiency of the $CB_1$ receptors expressed in specific cell types for a particular brain function (de Salas-Quiroga et al., 2015; Gutiérrez-Rodríguez et al., 2017; Lange et al., 2017; Remmers et al., 2017; Ruehle et al., 2013; Soria-Gómez et al., 2014). Importantly, knock-in mice with cell type-specific rescue of $CB_1$ receptors in dorsal telencephalic glutamatergic neurons (Glu-$CB_1$-RS) or GABAergic neurons (GABA-$CB_1$-RS) showed that the distribution pattern and the subcellular $CB_1$ receptor localization is maintained as it is observed in the wild-type hippocampus (Gutiérrez-Rodríguez et al., 2017; Remmers et al., 2017).

In this study, we hypothesized that intracellular $CB_1$ receptors are present in astroglial mitochondria as observed in neuronal and muscular mitochondria. The GFAP-$CB_1$-RS rescue mice expressing the $CB_1$ receptor gene exclusively in the astrocytes and the GFAPhrGFP-$CB_1$-WT mice are ideal genetic tools to test this hypothesis. Our results show that the subcellular $CB_1$ receptor distribution in astrocytes in the rescue mice completely matches the endogenous $CB_1$ receptor expression and localization in astrocytes of the wild-type mouse hippocampus. Moreover, our findings illustrate for the first time the localization of $CB_1$ receptors in astroglial mitochondria.

# 2 | MATERIALS AND METHODS

## 2.1 | Animal procedures

### 2.1.1 | Ethics statement

Experiments were approved by the Committee of Ethics for Animal Welfare of the University of the Basque Country UPV/EHU (CEIAB/2016/074, CEEA/M20/2016/073) and the Committee on Animal Health and Care of INSERM and the French Ministry of Agriculture and Forestry (authorization number, A501350). All animals were used according to the European Community Council Directive 2010/63/UE and the Spanish and French legislation (RD 53/2013 and Ley 6/2013). Maximal efforts were made in order to minimize the number and the suffering of the animals used.

### 2.1.2 | Conventional and conditional $CB_1$-KO

$CB_1$-KO mice were generated and genotyped as previously described (Marsicano et al., 2002). In addition, conditional $CB_1$ receptor mutant

mice were obtained by crossing the respective Cre expressing mouse line with $CB_1^{f/f}$ mice (Marsicano et al., 2003), using a three-step breeding protocol (Monory et al., 2006). Specifically, transgenic mice expressing the inducible version of the Cre recombinase CreERT2 under the control of the human glial fibrillary acid protein promoter, i.e. GFAP-CreERT2 mice (Hirrlinger, Scheller, Braun, Hirrlinger, & Kirchhoff, 2006) were crossed with mice carrying $CB_1$ receptor "floxed" sequence (Marsicano et al., 2003). As a result, transgenic mice $CB_1^{f/f;GFAP-CreERT2}$ were obtained (Han et al., 2012).

### 2.1.3 | Generation of GFAP-$CB_1$-RS

STOP-$CB_1$ mice were previously generated by inserting a loxP-flanked stop cassette into the 5′UTR of the coding exon of the $CB_1$ gene, 32 nucleotides upstream of the translational start codon (Ruehle et al., 2013). The STOP-$CB_1$ mice were crossed with GFAP-CreERT2 mice (Hirrlinger, Scheller, Braun, Hirrlinger, & Kirchhoff, 2006) to obtain $CB_1^{stop/stop;GFAP-CreERT2}$ mice.

Seven to nine-week-old $CB_1^{f/f;GFAP-CreERT2}$ and $CB_1^{f/f}$ littermates, as well as $CB_1^{stop/stop;GFAP-CreERT2}$ and $CB_1^{stop/stop}$ littermates were treated daily for eight consecutive days with 1 mg/kg (i.p.) of either tamoxifen or 4OH-tamoxifen synthesized as previously reported (Detsi, Koufaki, & Calogeropoulou, 2002; Yu & Forman, 2003) to induce the Cre-dependent astroglial deletion of $CB_1$ (GFAP-$CB_1$-KO and GFAP-$CB_1$-WT littermate mice) or its exclusive astroglial re-expression (rescue, GFAP-$CB_1$-RS and STOP-$CB_1$ littermates). Mice were used for immunocytochemistry 3–5 weeks after the last day of tamoxifen or 4OH-tamoxifen injections.

### 2.1.4 | Generation of GFAPhrGFP-$CB_1$-WT and GFAPhrGFP-$CB_1$-KO mice

Intrahippocampal injection of a recombinant adeno associated virus expressing hrGFP under the control of the human GFAP promoter (von Jonquieres et al., 2013) were performed in $CB_1$-WT and $CB_1$-KO mice to generate GFAPhrGFP-$CB_1$-WT and GFAPhrGFP-$CB_1$-KO, respectively. The vector backbone was the pAAV-GFAP-hChR2(H134R)-EYFP kindly provided by Karl Deisseroth (Stanford University, CA, USA). We replaced the hChR2(H134R)-EYFP with the cDNA encoding for hrGFP by using standard molecular cloning techniques. The virus production and purification, as well as the injection procedure were performed as previously described (Chiarlone et al., 2014). Coordinates for intrahippocampal injections were: anteroposterior – 2.0 mm, mediolateral ± 1.5 mm, dorsoventral – 2 mm relative to bregma. Mice were allowed to recover for at least 4 weeks after surgery before their anatomical characterization.

### 2.1.5 | Tissue isolation

Mice were housed under standard conditions (*ad libitum* food and water; 12hr/12hr light/dark cycle). $CB_1$-WT, GFAP-$CB_1$-RS, GFAP-$CB_1$-KO, $CB_1$-KO, STOP-$CB_1$, GFAPhrGFP-$CB_1$-WT and GFAPhrGFP-$CB_1$-KO mice (3 animals of each condition) were deeply anesthetized by intraperitoneal injection of ketamine/xylazine (80/10 mg/kg body weight) and transcardially perfused at room temperature (RT, 20°C–25°C) with phosphate buffered saline (.1 M PBS, pH 7.4) for 20 s,

followed by the fixative solution (4% formaldehyde freshly depolymerized from paraformaldehyde, .2% picric acid and .1% glutaraldehyde) in PBS (.1 M, pH 7.4) for 10–15 min. Brains were removed from the skull and post-fixed in the fixative solution for about 1 week at 4°C and stored at 4°C in 1:10 diluted fixative solution until use.

### 2.1.6 | Double pre-embedding immunogold and immunoperoxidase method for electron microscopy

Coronal hippocampal vibrosections were cut at 50 μm and collected in phosphate buffer (.1 M PB, pH 7.4) with .1% sodium azide at RT. They were transferred and pre-incubated in a blocking solution of 10% bovine serum albumin (BSA), .1% sodium azide and .02% saponine prepared in Tris-hydrogen chloride buffered saline 1× (TBS), pH 7.4 for 30 min at RT. Then, the $CB_1$-WT, GFAP-$CB_1$-RS, GFAP-$CB_1$-KO, $CB_1$-KO and STOP-$CB_1$ tissue sections were incubated with the primary goat polyclonal anti-$CB_1$ receptor antibody (2 μg/ml, #CB1-Go-Af450, Frontier Institute Co. Ltd, Ishikari, Hokkaido, Japan, RRID: AB_257130) and mouse monoclonal anti-GFAP antibody (1:1,000, #G3893, Sigma-Aldrich, St. Louis, MO, USA, RRID: AB_477010) diluted in 10% BSA/TBS containing .1% sodium azide and .004% saponine on a shaker for 2 days at 4°C. In parallel, GFAPhrGFP-$CB_1$-WT and GFAPhrGFP-$CB_1$-KO hippocampi were incubated with the same primary goat polyclonal anti-$CB_1$ receptor antibody as above and rabbit polyclonal anti-hrGFP antibody (1:500, #240142-51, Stratagene-Agilent, Santa Clara, CA, USA, RRID: AB_10598674) in 10% BSA/TBS with .1% sodium azide and .004% saponine for 2 days at 4°C.

The tissue was incubated after several washes in 1% BSA/TBS with the corresponding biotinylated secondary antibody (1:200 biotinylated anti-mouse, BA-2000; RRID:AB_2313581, and 1:200 biotinylated anti-rabbit BA-1000; RRID:AB_2313606, Vector Labs, Burlingame, CA, USA) in 1% BSA/TBS with .004% saponine for 3 hr at RT. The sections were washed in 1% BSA/TBS overnight on a shaker at 4°C, incubated with the secondary 1.4 nm gold-labeled immunoglobulin-G antibody (Fab' fragment, 1:100, Nanoprobes Inc., Yaphank, NY, USA) in 1% BSA/TBS with .004% saponine on a shaker for 3 hr at RT, washed in 1% BSA/TBS and subsequently incubated in the avidin-biotin complex (1:50; PK-7100, Vector Labs, Burlingame, CA, USA) diluted in the wash solution for 1.5 hr. After washing the sections in 1% BSA/TBS overnight at 4°C, they were post-fixed with 1% glutaraldehyde in TBS for 10 min and washed in double-distilled water. Then, the gold particles were silver-intensified with a HQ Silver kit (Nanoprobes Inc., Yaphank, NY, USA) for about 12 min in the dark, washed in .1 M PB (pH 7.4) and subsequently incubated in .05% diaminobenzidine (DAB) and .01% hydrogen peroxide prepared in .1 M PB for 3 min. Finally, the sections were osmicated (1% osmium tetroxide, in .1 M PB pH 7.4) for 20 min, washed in .1 M PB (pH 7.4), dehydrated in graded alcohols (50%–100%) to propylene oxide and plastic-embedded in Epon resin 812. 50-60 nm-ultrathin sections were cut with a diamond knife (Diatome USA), collected on nickel mesh grids or on formvar-coated single slot grids for serial sectioning, stained with 2.5% lead citrate, and examined with a Philips EM208S electron microscope. Tissue preparations were photographed by means of a digital camera coupled to the electron microscope. Minor adjustments in contrast and

brightness were made to the figures using Adobe Photoshop (Adobe Systems, San Jose, CA, USA). GIMP (GNU Project) and Adobe Photoshop were used to blend the electron micrographs into the serial photocomposition.

### 2.1.7 | Semi-quantification of the $CB_1$ receptor immunogold and immunoperoxidase staining

The pre-embedding immunogold and immunoperoxidase methods were simultaneously applied and repeated three times on the sections obtained from each of the three individual $CB_1$-WT, GFAP-$CB_1$-RS, GFAP-$CB_1$-KO, $CB_1$-KO, STOP-$CB_1$, GFAPhrGFP-$CB_1$-WT and GFAPhrGFP-$CB_1$-KO animals studied. Immunogold-labeling was visualized on the hippocampal sections with a light microscope and portions of the CA1 stratum radiatum and the dentate molecular layer with good and consistent $CB_1$ receptor immunolabeling were identified and trimmed down for ultrathin sectioning. Three to four semi-thin sections (1 μm-thick) were then cut with a histo-diamond knife (Diatome USA) and stained with 1% toluidine blue. To further standardize the conditions, only the first 20 ultrathin sections (60 nm thick) were cut, collected onto the grids and photographed. The electron micrographs were taken at 18,000× with a Digital Morada Camera from Olympus (Hamburg, Germany). Sampling was always carefully and accurately carried out in the same way for all the animals studied and it was blinded to experimenters during $CB_1$ receptor quantification.

Positive astrocytic processes were identified by the presence of DAB immunodeposits. Positive $CB_1$ receptor labeling was considered if at least one immunoparticle was within ~30 nm of the plasmalemma or outer mitochondrial membranes. Furthermore, only particles on mitochondrial membrane segments far away from other astrocytic membranes (distance ≥80 nm) and well distinct from the astrocytic intermediate filaments or any other intracellular organelle membranes were taken into account for mitochondrial localization. Image-J software (NIH; RRID:SCR_003070) was used to measure the membrane length. Percentages of $CB_1$ receptor positive profiles (astrocytic processes and mitochondria), density (particles/μm membrane), the proportion of $CB_1$ receptor particles in astrocytes versus total $CB_1$ receptor expression and the proportion of $CB_1$ receptor particles in terminals versus total $CB_1$ receptor expression in plasmalemma, were analyzed and displayed as mean ± SEM using a statistical software package (GraphPad Prism 5, GraphPad Software Inc, San Diego, USA; RRID: SCR_002798). The normality test (Kolmogorov-Smirnov normality test) was applied before statistical tests and subsequently data were analyzed using nonparametric tests (Mann-Whitney $U$ test when $k = 2$ or Kruskal-Wallis test when $k > 2$). Potential variability between animals of the same mutant mouse line was assessed statistically. Because no differences were detected, all data within each mouse line were pooled.

### 2.1.8 | Semi-quantification of the distance from the $CB_1$ receptor particles in astroglial mitochondria to the nearest synapse

Image-J software was used to measure the distance between the $CB_1$ receptor immunogold particles on the astrocytic mitochondria and the nearest synapse on single 60 nm-thick sections. Data were tabulated,

analyzed and displayed as mean ± SEM using GraphPad Prism 5 software.

## 3 | RESULTS

### 3.1 | Subcellular $CB_1$ receptor localization in the mutant mice

Astrocytes and their processes were identified by DAB immunodeposits of GFAP or hrGFP and the $CB_1$ receptor was detected by immunogold labeling. As expected, the $CB_1$ receptor was mainly localized on neuronal terminals, preterminal membranes and, to a lesser extent, on GFAP-labeled astrocytes. $CB_1$ receptor-immunopositive synaptic terminals followed in serial ultrathin sections obtained from the CA1 (Figure 1) and dentate molecular layer (Figure 2) of the $CB_1$-WT mouse could be found adjacent to double-labeled GFAP and $CB_1$ receptor-immunopositive astrocytic processes (Figures 1–3a and 4a) that also contained $CB_1$ receptor-immunopositive mitochondria (Figures 1–4). In GFAP-$CB_1$-RS hippocampus, the $CB_1$ receptor immunolabeling was restricted to the DAB-containing astrocytic elements and no labeling was found on axon boutons (Figures 3c and 4c). Conversely, the $CB_1$ receptor particles in the GFAP-$CB_1$-KO hippocampus were only on synaptic terminals but not in astrocytic processes (Figures 3d and 4d). Also, $CB_1$ receptor immunoparticles were found in neuronal mitochondria but not in mitochondria of astrocytes in the GFAP-$CB_1$-KO (Figure 3d). Finally, the subcellular distribution of the $CB_1$ receptor on synaptic terminals and astrocytic elements of the GFAPhrGFP-$CB_1$-WT resembled the $CB_1$-WT hippocampus (Figures 3f,g and 4f,g). Importantly, this $CB_1$ receptor staining pattern was absent in $CB_1$-KO (Figures 3b and 4b), STOP-$CB_1$ (Figures 3e and 4e) and GFAPhrGFP-$CB_1$-KO mice (Figures 3h and 4h).

### 3.2 | $CB_1$ receptor assessment in astrocytes of the CA1 stratum radiatum

The percentage of the $CB_1$ receptor immunopositive astrocytic processes in the CA1 stratum radiatum of the GFAP-$CB_1$-RS (37.12% ± 3.79%) was not statistically different ($p > .05$; Figure 5a) relative to the $CB_1$-WT mouse (42.06% ± 3.56%), however the proportion in the GFAPhrGFP-$CB_1$-WT was significantly higher (59.91% ± 3.29%; ***$p < .001$; Figure 5a). Only background metal particles were found in CA1 astrocytes of the STOP-$CB_1$, GFAP-$CB_1$-KO, $CB_1$-KO and GFAPhrGFP-$CB_1$-KO mice (***$p < .001$; Figure 5a).

The density of $CB_1$ receptor immunoparticles on astrocytic membranes (particles/μm) was also analyzed (Figure 5b). Similar densities were detected in the GFAP-$CB_1$-RS (.128 ± .020) and the $CB_1$-WT (.135 ± .019; $p > .05$; Figure 5b) however the density was much higher in the GFAPhrGFP-$CB_1$-WT (.384 ± .039; ***$p < .001$; Figure 5b). Only residual non-specific particles were observed in the STOP-$CB_1$ (.005 ± .003), GFAP-$CB_1$-KO (.005 ± .003), $CB_1$-KO (.001 ± .001) and GFAPhrGFP-$CB_1$-KO mice (.004 ± .002; ***$p < .001$; Figure 5b).

5.31% ± .84% of the total $CB_1$ receptor labeling in the $CB_1$-WT, 11.97% ± 2.17% in the GFAPhrGFP-$CB_1$-WT ($p > .05$; Figure 5c) and
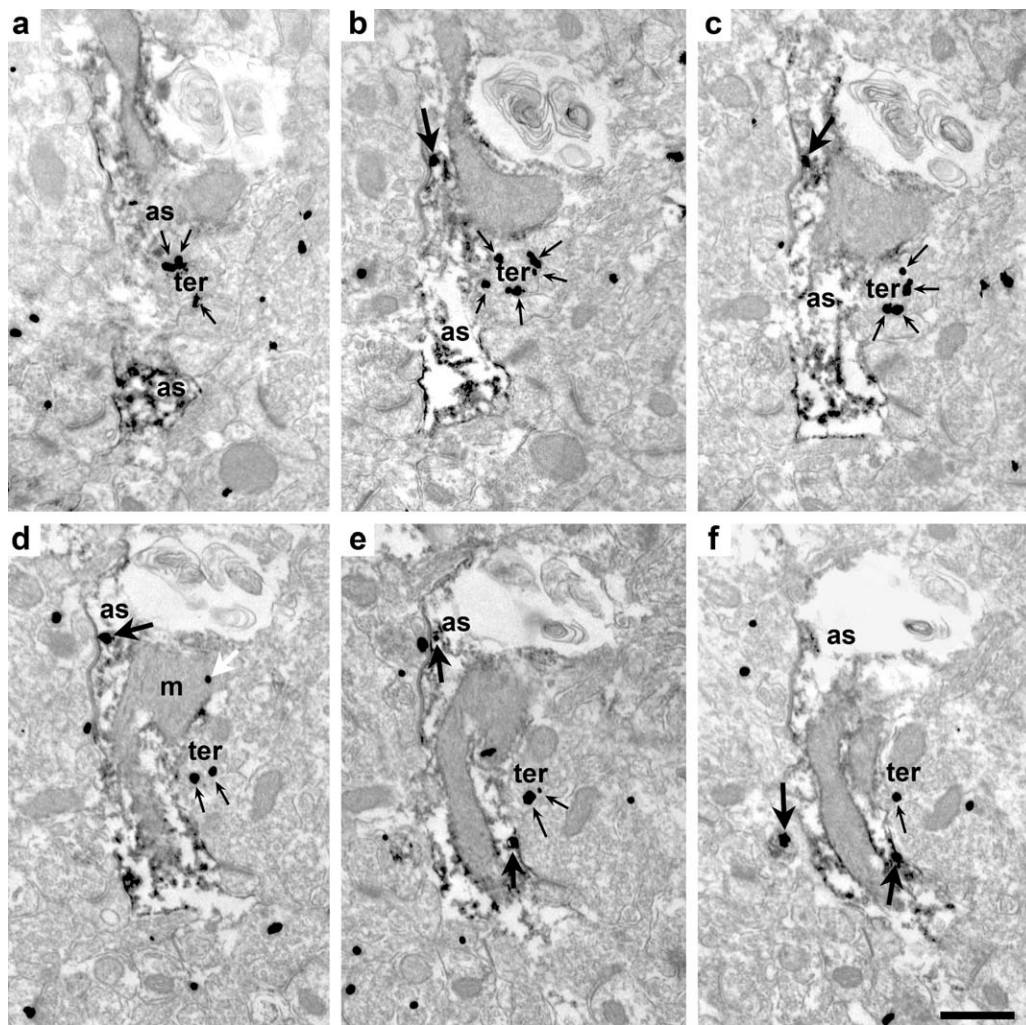
**FIGURE 1** Follow up of a CB$_1$ receptor positive astrocytic process in the CA1 stratum radiatum of CB$_1$-WT. Double pre-embedding immunogold (CB$_1$ receptor) and immunoperoxidase (GFAP) method for electron microscopy. Serial ultrathin sections showing a GFAP positive (DAB immunodeposits) astrocytic process (as) with a few CB$_1$ receptor immunoparticles on the astrocytic membrane throughout the reconstruction (b–f). In the astrocyte, CB$_1$ receptor labeling is also observed on the mitochondrial membrane (d). A CB$_1$ receptor-positive terminal (ter) is closely associated to the astrocytic process. Black thin arrows: neuronal CB$_1$ receptor labeling; black thick arrows: astrocytic CB$_1$ receptor labeling; white arrow: mitochondrial CB$_1$ receptor labeling in astrocyte; as: astrocytic process; ter: axon terminal; m: CB$_1$ receptor-positive mitochondria in astrocyte. Scale bar: 0.5 μm

95.31% ± 1.87% in the GFAP-CB$_1$-RS were in astrocytic processes (***$p < .001$; Figure 5c). Only background immunoparticles were detected in astrocytic processes of the STOP-CB$_1$, GFAP-CB$_1$-KO, CB$_1$-KO and GFAPhrGFP-CB$_1$-KO (***$p < .001$; Figure 5c). As a comparison, 65.52% ± 2.44% of the total CB$_1$ receptor gold particles in the CB$_1$-WT, 75.13% ± 4.06% in the GFAP-CB$_1$-KO and 56.32% ± 2.73% in the GFAPhrGFP-CB$_1$-WT were distributed on synaptic terminals ($p > .05$; Figure 5d). Scattered metal particles were found in GFAP-CB$_1$-RS, STOP-CB$_1$, CB$_1$-KO and GFAPhrGFP-CB$_1$-KO mice (***$p < .001$; Figure 5d).

## 3.3 | CB$_1$ receptor assessment in astrocytes of the dentate molecular layer

The proportion of the CB$_1$ receptor immunopositive astrocytic processes in the GFAP-CB$_1$-RS (39.84% ± 3.50%) and the CB$_1$-WT (44.67% ± 3.85%) was statistically similar ($p > .05$; Figure 6a), but it was significantly higher in the GFAPhrGFP-CB$_1$-WT group (59.99% ± 3.37%; **$p < .01$; Figure 6a). Particles were virtually undetectable in the STOP-CB$_1$, GFAP-CB$_1$-KO, CB$_1$-KO and GFAPhrGFP-CB$_1$-KO mice (***$p < .001$; Figure 6a).

The CB$_1$ receptor density (particles/μm) on astrocytic membranes did not differ statistically between the GFAP-CB$_1$-RS (.138 ± .016) and the CB$_1$-WT (.112 ± .011; $p > .05$; Figure 6b) but it was higher in the GFAPhrGFP-CB$_1$-WT group (.334 ± .033; ***$p < .001$; Figure 6b). Negligible particle numbers were noticed in the STOP-CB$_1$ (.006 ± .003), GFAP-CB$_1$-KO (.006 ± .003), CB$_1$-KO (.004 ± .002) and GFAPhrGFP-CB$_1$-KO (.002 ± .002; ***$p < .001$; Figure 6b).

Of the total CB$_1$ receptor labeling, 5.35% ± 1.00% in the CB$_1$-WT, 13.13% ± 2.60% in the GFAPhrGFP-CB$_1$-WT ($P > .05$; Figure 6c) and 95.61% ± 1.56% in the GFAP-CB$_1$-RS was in astrocytes (***$P < .001$; Figure 6c). Non-specific CB$_1$ receptor immunoparticles were found on
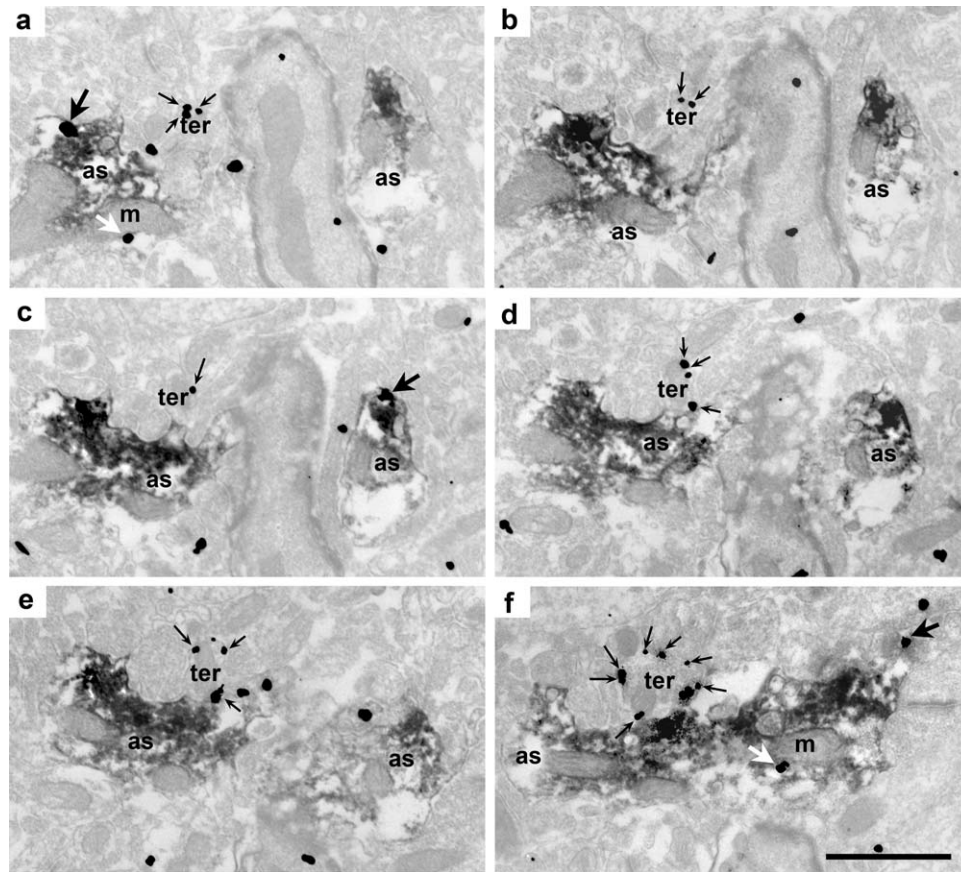
**FIGURE 2** Follow up of a $CB_1$ receptor-positive astrocytic process in the dentate molecular layer of $CB_1$-WT. Double pre-embedding immunogold ($CB_1$ receptor) and immunoperoxidase (GFAP) method for electron microscopy. Serial ultrathin sections showing a GFAP positive (DAB immunodeposits) astrocytic process (as) with scattered $CB_1$ receptor immunoparticles on the astrocytic (a,c,f) and mitochondrial (a,f) membranes. A $CB_1$ receptor-positive synaptic terminal (ter) is related to the astrocytic process. Black thin arrows: neuronal $CB_1$ receptor labeling; black thick arrows: astrocytic $CB_1$ receptor labeling; white arrows: mitochondrial $CB_1$ receptor labeling in astrocyte; as: astrocytic process; ter: axon terminal; m: $CB_1$ receptor-positive mitochondria in astrocyte. Scale bar: 1 μm

astrocytic processes in the STOP-$CB_1$, GFAP-$CB_1$-KO, $CB_1$-KO and GFAPhrGFP-$CB_1$-KO mice (***$P < .001$; Figure 6c). Conversely, 64.27% ± 2.88% of the total $CB_1$ receptor labeling in the $CB_1$-WT, 76.17% ± 4.70% in the GFAP-$CB_1$-KO and 57.17% ± 2.19% in the GFAPhrGFP-$CB_1$-WT was located on synaptic terminals ($P > .05$; Figure 6d). Residual metal particles were detected in the GFAP-$CB_1$-RS, STOP-$CB_1$, $CB_1$-KO and GFAPhrGFP-$CB_1$-KO (***$P < .001$; Figure 6d).

## 3.4 | $CB_1$ receptor localization in astroglial mitochondria

$CB_1$ receptor labeling was observed in mitochondria (mt$CB_1$ receptors) of astrocytes distributed throughout the CA1 stratum radiatum (Figures 1d and 3a,c,g) and dentate molecular layer (Figures 2a,f and 4a,c,f,g). In $CB_1$-WT mice, 11.12% ± 1.80% of the astrocytic mitochondrial sections in the CA1 stratum radiatum and 11.56% ± 2.33% in the dentate molecular layer were $CB_1$ receptor immunopositive (Figures 7a,b). The percentage was roughly similar in GFAP-$CB_1$-RS (CA1 stratum radiatum: 12.39% ± 1.81% ($p > .05$; Figure 7a); dentate molecular layer: 11.48% ± 1.76% ($p > .05$; Figure 7b) and GFAPhrGFP-$CB_1$-WT (CA1 stratum radiatum: 13.12% ± 2.53% ($P > .05$; Figure 7a); dentate

molecular layer: 13.74% ± 3.20% ($p > .05$; Figure 7b). Non-specific mitochondrial particles were detected in STOP-$CB_1$ (CA1 stratum radiatum: 4.66% ± 1.55%, **$p < .01$; Figure 7a; dentate molecular layer: 5.38% ± 1.22%, *$p < .05$; Figure 7b), GFAP-$CB_1$-KO (CA1 stratum radiatum: 3.97% ± 1.70%, **$p < .01$; Figure 7a; dentate molecular layer: 3.04% ± 1.04%, **$p < .01$; Figure 7b), $CB_1$-KO (CA1 stratum radiatum: 2.97% ± 1.15%. ***$p < .001$; Figure 7a; dentate molecular layer: 2.49% ± .80%, ***$p < .001$; Figure 7b) and GFAPhrGFP-$CB_1$-KO mice (CA1 stratum radiatum: .95% ± .95%, ***$p < .001$; Figure 7a; dentate molecular layer: 1.98% ± .91%, ***$p < .001$; Figure 7b).

## 3.5 | Distance from the astroglial mt$CB_1$ receptors to the nearest synapse

The distance between the astrocytic mt$CB_1$ receptor particles and the midpoint of the nearest synapse was assessed in $CB_1$-WT, GFAP-$CB_1$-RS and GFAPhrGFP-$CB_1$-WT hippocampi (Figure 8; table 1). In the CA1, 10.55% ± 4.01% of the total synapses analyzed were in a range of 0–400 nm from the astrocytic mt$CB_1$ receptor particles in $CB_1$-WT, 2.67% ± 2.67% in GFAP-$CB_1$-RS and 7.41% ± 3.70% in GFAPhrGFP-$CB_1$-WT. 38.54% ± 8.32% of the synapses were located between 400
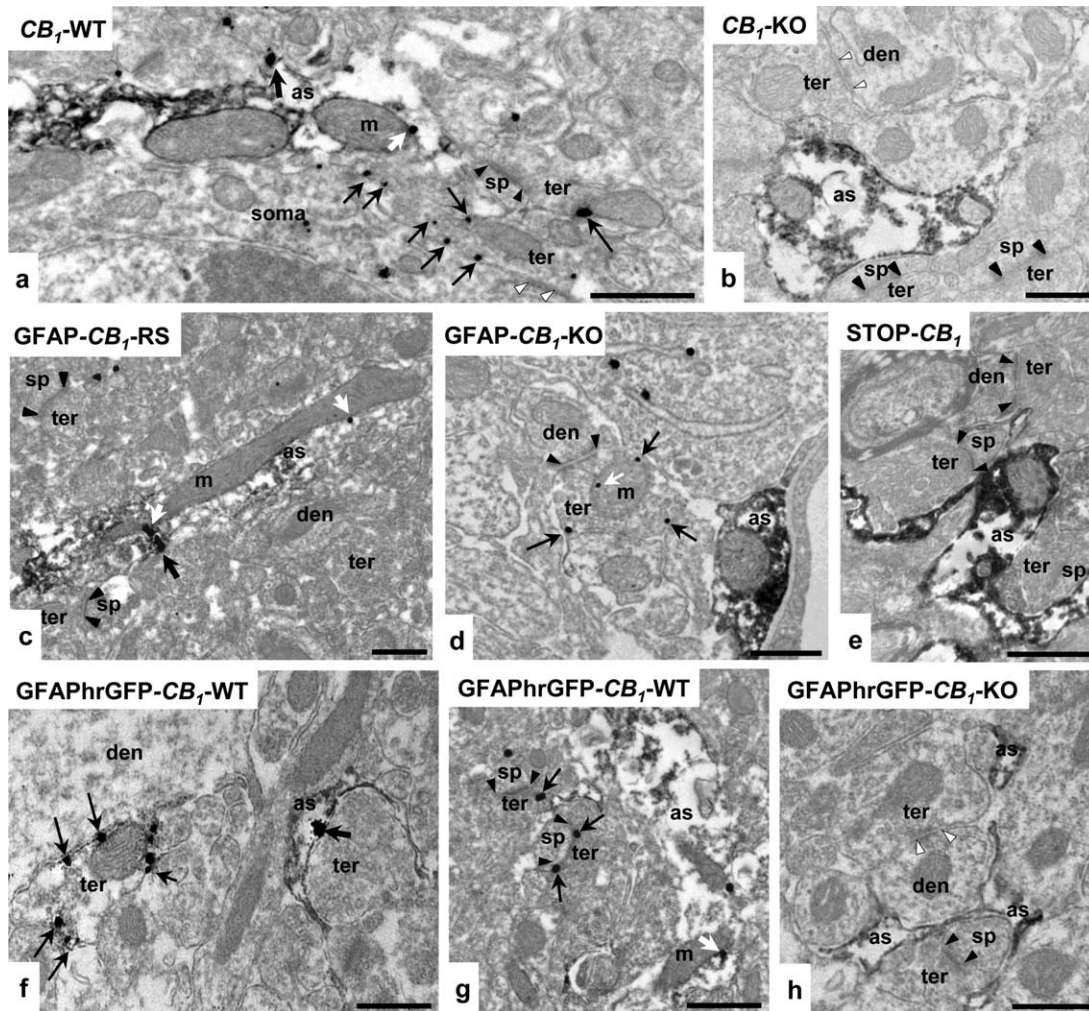
**FIGURE 3** $CB_1$ receptor localization in identified astrocytes and astrocytic mitochondria in the CA1 stratum radiatum of mutant mice. Pre-embedding immunogold and immunoperoxidase method for electron microscopy. In $CB_1$-WT (a), $CB_1$ receptor immunoparticles are localized on membranes of astrocytic processes. Mitochondrial $CB_1$ receptor labeling is also visualized in identified astrocytes of $CB_1$-WT (a). As expected, $CB_1$ receptor immunoparticles are also on membranes of synaptic terminals and preterminals (a). No $CB_1$ receptor immunolabeling is detected in $CB_1$-KO (b), confirming the specificity of the $CB_1$ receptor antibody. Astrocytic processes, but not axon terminals, are $CB_1$ receptor immunopositive in GFAP-$CB_1$-RS (c). Note in this mutant, $CB_1$ receptor labeling on the outer membrane of an astrocytic mito-chondrion (c). $CB_1$ receptor particles are found in synaptic terminals and neuronal mitochondria, but not in astrocytes and astrocytic mito-chondria, of GFAP-$CB_1$-KO (d). No $CB_1$ receptor immunoparticles are observed in STOP-$CB_1$ (e). In GFAPhrGFP-$CB_1$-WT (f and g), presynaptic terminals and astrocytic processes are $CB_1$ receptor positive. Mitochondrial $CB_1$ receptor labeling is also visualized in identified astrocytes (g). No $CB_1$ receptor immunolabeling is detected in GFAPhrGFP-$CB_1$-KO (h). Black arrowheads: excitatory synapses; white arrow-heads: inhibitory synapses; black thin arrows: neuronal $CB_1$ receptor immunoparticles; black thick arrows: astrocytic $CB_1$ receptor immuno-particles; white thick arrows: mitochondrial $CB_1$ receptor labeling in astrocytes; white thin arrows: mitochondrial $CB_1$ receptor labeling in neurons; as: astrocytic processes; ter: terminal; den: dendrite; sp: dendritic spine; m: $CB_1$ receptor-positive astroglial/neuronal mitochondria. Scale bars: 0.5 $\mu$m

and 800 nm in $CB_1$-WT, 49.28% ± 2.87% in GFAP-$CB_1$-RS and 51.85% ± 3.70% in GFAPhrGFP-$CB_1$-WT. 29.51% ± 6.85% of the synapses were detected between 800 and 1,200 nm in $CB_1$-WT, 37.26% ± 2.02% in GFAP-$CB_1$-RS and 29.63% ± 7.41% in GFAPhrGFP-$CB_1$-WT. Finally, 21.40% ± 5.56% of the synapses were found at more than 1,200 nm from the astrocytic mt$CB_1$ receptor in $CB_1$-WT, 10.79% ± 2.94% in GFAP-$CB_1$-RS and 14.81% ± 7.41% in GFAPhrGFP-$CB_1$-WT (Figure 8; Table 1). In the dentate molecular layer, 11.11% ± 6.42% of the total synapses analyzed were at 0–400 nm in $CB_1$-WT, 2.82% ± 1.48% in GFAP-$CB_1$-RS and 1.52% ±

1.52% in GFAPhrGFP-$CB_1$-WT. 50% ± 3.21% of the synapses were located at a distance of between 400 and 800 nm from the astrocytic mt$CB_1$ immunoparticle in $CB_1$-WT, 47.57% ± 4.81% in GFAP-$CB_1$-RS and 57.37% ± 6.26% in GFAPhrGFP-$CB_1$-WT. 23.15% ± .93% of them were located between 800 and 1,200 nm in $CB_1$-WT, 43.79% ± 3.13% in GFAP-$CB_1$-RS and 35.86% ± 2.53% in GFAPhrGFP-$CB_1$-WT. Finally, 18.52% ± 3.70% of the synapses in $CB_1$-WT, 11.82% ± 3.51% in GFAP-$CB_1$-RS and 5.25% ± 2.72% in GFAPhrGFP-$CB_1$-WT were observed at more than 1,200 nm from the astrocytic mt$CB_1$ receptor particles (Figure 8; Table 1).
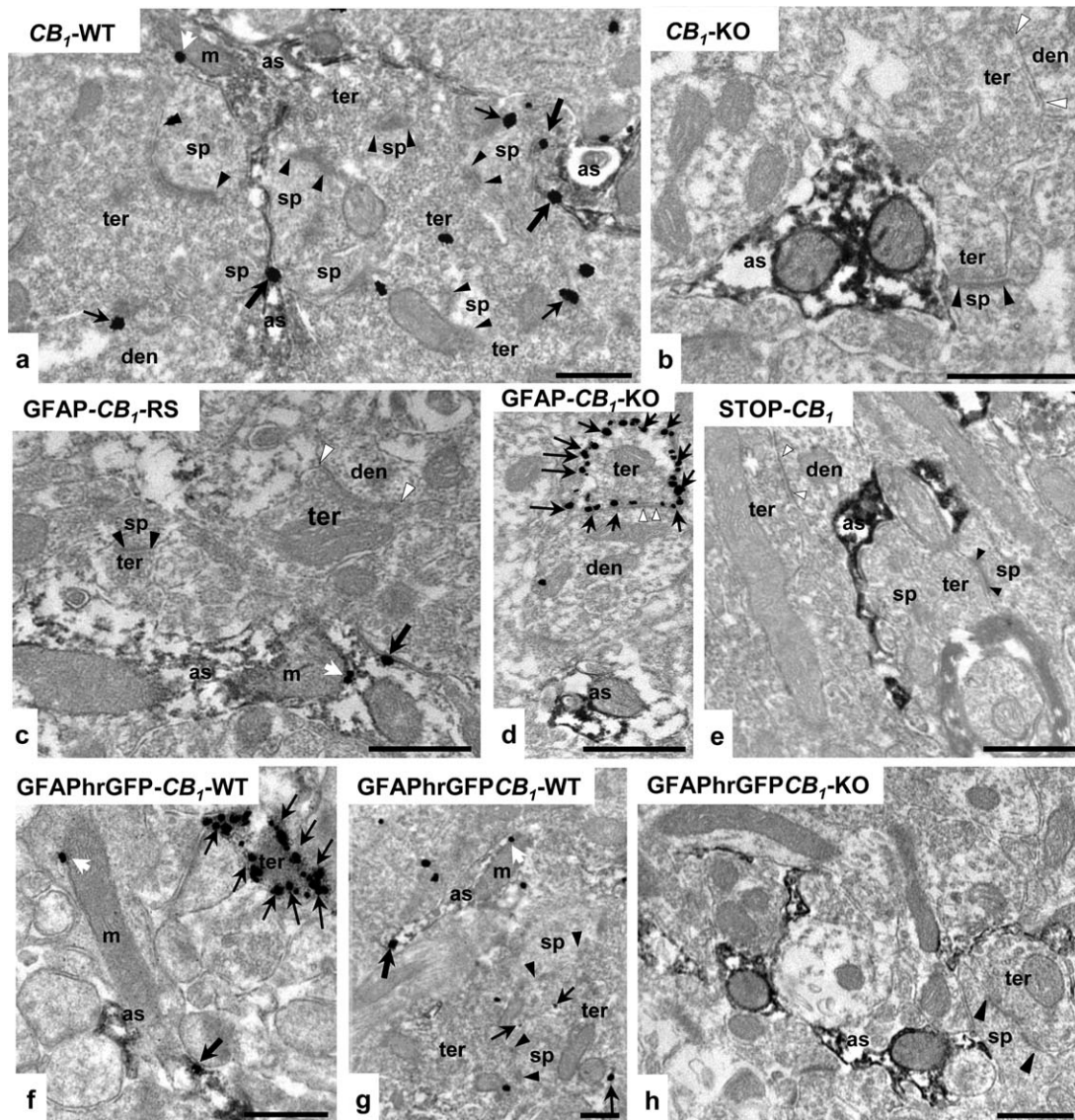
**FIGURE 4** CB$_1$ receptor localization in identified astrocytes and astrocytic mitochondria in the dentate molecular layer of mutant mice. Pre-embedding immunogold and immunoperoxidase method for electron microscopy. In *CB$_1$*-WT, CB$_1$ receptor immunoparticles are localized on membranes of presynaptic terminals, astrocytic processes as well as on mitochondrial membranes of identified astrocytes (a). Importantly, the CB$_1$ receptor labeling is absent in *CB$_1$*-KO (b). In GFAP-*CB$_1$*-RS, CB$_1$ receptor gold particles are only detected on astrocytes and astrocytic mitochondria but not on neuronal synaptic compartments (c). Conversely, CB$_1$ receptor immunolabeling is only present on synaptic boutons and not on astrocytes of GFAP-*CB$_1$*-KO (d). The CB$_1$ receptor labeling is not observed in the STOP-*CB$_1$* mouse (e). In GFAPhrGFP-*CB$_1$*-WT, CB$_1$ receptor immunoparticles are localized on membranes of presynaptic terminals, astrocytic processes and astrocytic mitochondria (f and g). No CB$_1$ receptor immunolabeling is detected in GFAPhrGFP-*CB$_1$*-KO (h). Black arrowheads: excitatory synapses; white arrowheads: inhibitory synapses; black thin arrows: neuronal CB$_1$ receptor immunoparticles; black thick arrows: astrocytic CB$_1$ receptor immunoparticles; white arrows: mitochondrial CB$_1$ receptor labeling in astrocytes; as: astrocytic processes; ter: terminal; den: dendrite; sp: dendritic spine; m: CB$_1$ receptor-positive astrocytic mitochondria. Scale bars: 0.5 μm

## 4 | DISCUSSION

The high CB$_1$ receptor expression in the hippocampus is unevenly distributed between subcellular compartments of GABAergic and glutamatergic synaptic terminals, astrocytes and neuronal mitochondria (Bénard et al., 2012; Gutiérrez-Rodríguez et al., 2017; Han et al., 2012; Hebert-Chatelain et al., 2014a,b, 2016; Katona & Freund, 2012; Lu & Mackie, 2016; Marsicano & Lutz, 1999; Steindel et al., 2013). However, no information is available to date whether the CB$_1$ receptor localizes

in astroglial mitochondria as it does in mitochondria of hippocampal GABAergic and glutamatergic neurons (Bénard et al., 2012; Hebert-Chatelain et al., 2014a,b, 2016). In order to address this, we used conditional CB$_1$ receptor rescue mice re-expressing the CB$_1$ receptor exclusively in astrocytic GFAP expressing cells (GFAP-*CB$_1$*-RS), as well as *CB$_1$*-WT and *CB$_1$*-KO mice expressing hrGFP (De Francesco et al., 2015; Hadaczek et al., 2009; Kerr et al., 2015; Navarro-Galve et al., 2005; Ward & Cormier, 1979) under the control of the GFAP promoter (GFAPhrGFP-*CB$_1$*-WT and GFAPhrGFP-*CB$_1$*-KO, respectively). As a
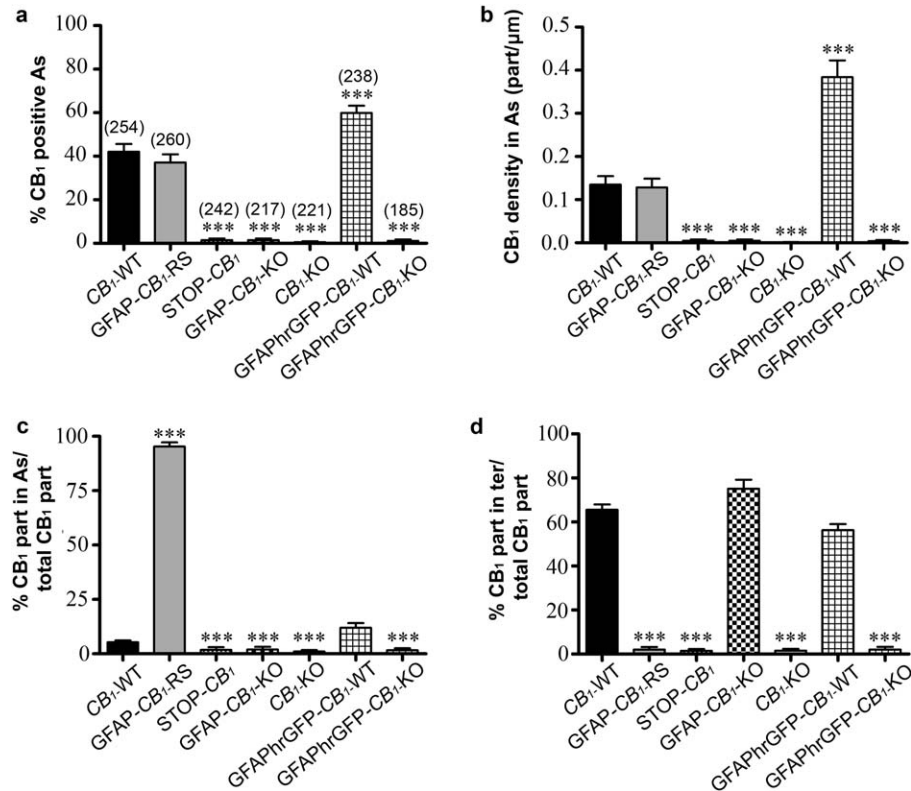
**FIGURE 5** Statistical assessment of the $CB_1$ receptor distribution on astrocytes in the CA1 stratum radiatum of the mutant mice. (a). Percentages of $CB_1$ receptor immunopositive astrocytic processes in $CB_1$-WT (42.06% ± 3.56%) and GFAP-$CB_1$-RS (37.12% ± 3.79%) do not show statistical differences. The proportion of 59.91% ± 3.29% in GFAPhrGFP-$CB_1$-WT is statistically significant. Only residual background is found in STOP-$CB_1$ (1.46% ± .78%), GFAP-$CB_1$-KO (1.45% ± .77%), $CB_1$-KO (.54% ± .39%) and GFAPhrGFP-$CB_1$-KO (1.16% ± .67%). The number of astrocytic processes examined is in parentheses on the top of each column. (b). $CB_1$ receptor immunoparticle density on membranes of astrocytic processes (particles/μm). Densities in $CB_1$-WT (.135 ± .019) and GFAP-$CB_1$-RS (.128 ± .020) are statistically similar, whereas a significant increase in particle density is found in GFAPhrGFP-$CB_1$-WT (.384 ± .039). Non-specific particles are detected in STOP-$CB_1$ (.005 ± .003), GFAP-$CB_1$-KO (.005 ± .003), $CB_1$-KO (.001 ± .001) and GFAPhrGFP-$CB_1$-KO (.004 ± .002). (c) Proportion of $CB_1$ receptor gold particles on astrocytic membranes versus total $CB_1$ receptor expression on plasmalemma: 5.31% ± .84% of the total $CB_1$ receptor immunoparticles are located in astrocytes of $CB_1$-WT and 95.31% ± 1.87% in astrocytes of GFAP-$CB_1$-RS. Only residual $CB_1$ immunoparticles are in astrocytic processes of STOP-$CB_1$ (1.76% ± 1.29%), GFAP-$CB_1$-KO (1.96% ± 1.28%), $CB_1$-KO (1.02% ± .72%) and GFAPhrGFP-$CB_1$-KO (1.62% ± .94%). (d) Proportion of immunogold particles on synaptic terminals versus total $CB_1$ receptor expression on plasmalemma: 65.52% ± 2.44% ($CB_1$-WT), 75.13% ± 4.06% (GFAP-$CB_1$-KO), and 56.32% ± 2.73% (GFAPhrGFP-$CB_1$-WT). Residual $CB_1$ receptor immunoparticles are in astrocytes of GFAP-$CB_1$-RS (2.02% ± 1.17%), STOP-$CB_1$ (1.47% ± .84%), $CB_1$-KO (1.52% ± .87%) and GFAPhrGFP-$CB_1$-KO (2.08% ± 1.19%). Data are expressed as mean ± SEM of three different animals. Data were analyzed by means of Kruskal-Wallis Test and the Dunn's Multiple Comparison Post-hoc test. ***$p < .001$; **$p < .01$; *$p < .05$. As: astrocytic processes; ter: terminal; part: immunoparticles

first step, we determined the $CB_1$ receptor expression and distribution in the conditional mutant mice in order to draw the level of agreement with the $CB_1$ receptor expression pattern in the $CB_1$-WT mice. The combined pre-embedding immunogold and immunoperoxidase method applied in this study has been previously proven to be an excellent approach for the localization of the $CB_1$ receptor in astrocytes (Bonilla-Del Río et al., 2017; Bosier et al., 2013; Han et al., 2012) and mitochondria (Bénard et al., 2012; Hebert-Chatelain et al., 2014a,b, 2016). Specificity control experiments of the $CB_1$ receptor antibodies were carried out in $CB_1$-KO and STOP-$CB_1$ mice (carrying a loxP-flanked stop cassette inserted into the sequences of the 5'UTR of the $CB_1$ receptor). According to recent observations, we detected very low levels of metal particle deposits in STOP-$CB_1$ (Remmers et al., 2017) and scattered background particles in $CB_1$-KO.

The results showed that the proportion and density of the $CB_1$ receptor immunolabeling (particles/μm) of astrocytic processes in the hippocampus were not significantly different between GFAP-$CB_1$-RS and $CB_1$-WT. The percentage of immunopositive astrocytes in CA1 of $CB_1$-WT was in the range of the previous values reported by our group (Bonilla-Del Río et al., 2017; Han et al., 2012), and almost all of the $CB_1$ receptor labeling was expressed in astrocytic elements in GFAP-$CB_1$-RS. Furthermore, the proportion of astrocytic processes expressing $CB_1$ receptors and the density of receptor particles were about 34% and 64% higher, respectively, in the mutant mice targeted to express hrGFP in astroglial cells (GFAPhrGFP-$CB_1$-WT) than in GFAP-$CB_1$-RS. These results suggest that the $CB_1$ receptor expression in astrocytes could actually be higher than previously reported using the astrocytic GFAP marker (Bosier et al., 2013; Han et al., 2012), because the GFAP
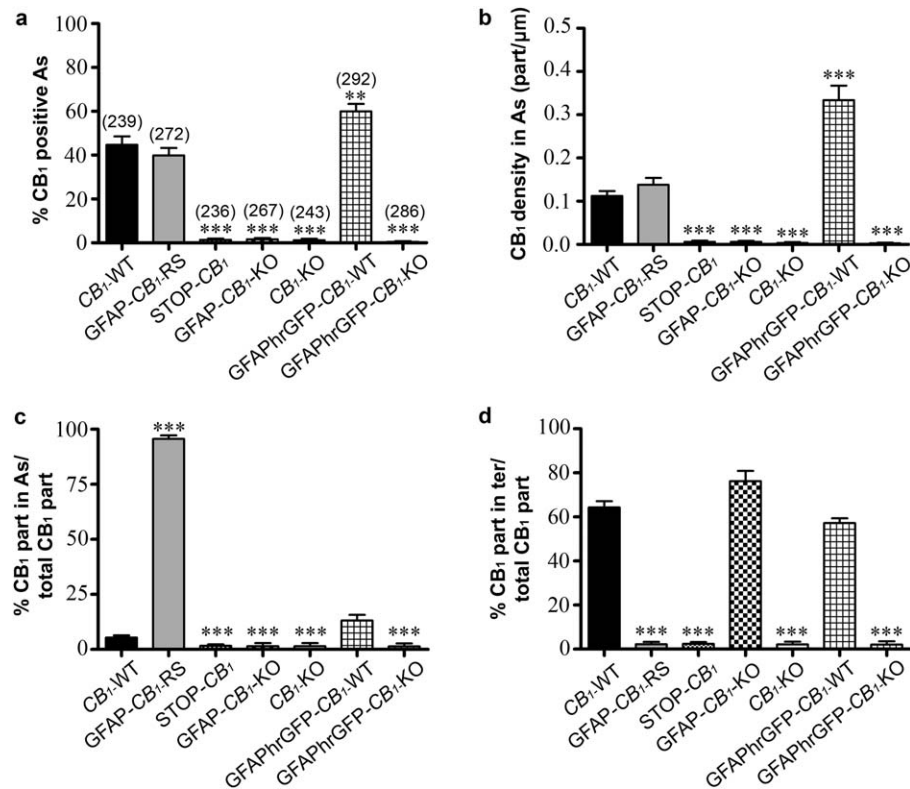
**FIGURE 6** Statistical assessment of the $CB_1$ receptor distribution on astrocytes in the dentate molecular layer of the mutant mice. (a). Similar percentages of $CB_1$ receptor immunopositive astrocytic processes in $CB_1$-WT (44.67% $\pm$ 3.85%) and GFAP-$CB_1$-RS (39.84% $\pm$ 3.50%) are found. Statistical differences are obtained in GFAPhrGFP-$CB_1$-WT (59.99% $\pm$ 3.37%). Just residual particles are in: STOP-$CB_1$ (1.33% $\pm$ .64%), GFAP-$CB_1$-KO (1.59% $\pm$ .66%), $CB_1$-KO (1.19% $\pm$ .71%) and GFAPhrGFP-$CB_1$-KO (.47% $\pm$ .36%). The number of astrocytic processes studied is in parentheses on the top of each column. (b) Analysis of $CB_1$ receptor density (particles/$\mu$m) on astrocytic processes shows no statistical differences between $CB_1$-WT (.112 $\pm$ .011) and GFAP-$CB_1$-RS (.138 $\pm$ .016); however, the density on GFAPhrGFP-$CB_1$-WT (.334 $\pm$ .033) is statistically higher. Only residual background is counted in STOP-$CB_1$ (.006 $\pm$ .003), GFAP-$CB_1$-KO (.006 $\pm$ .003), $CB_1$-KO (.004 $\pm$ .002) and GFAPhrGFP-$CB_1$-KO (.002 $\pm$ .002). (c) Proportion of $CB_1$ receptor immunoparticles on astrocytic membranes versus total $CB_1$ receptor expression on plasmalemma: 5.35% $\pm$ 1.00% ($CB_1$-WT), 95.61% $\pm$ 1.56% (GFAP-$CB_1$-RS). Almost null non-specific immunoparticles are found in STOP-$CB_1$ (1.65% $\pm$ .66%), GFAP-$CB_1$-KO (1.45% $\pm$ 1.45%), $CB_1$-KO (1.43% $\pm$ 1.43%) and GFAPhrGFP-$CB_1$-KO (1.37% $\pm$ 1.37%). (d) Proportion of immunogold particles localized on synaptic terminals versus total $CB_1$ receptor expression on plasmalemma: 64.27% $\pm$ 2.88% ($CB_1$-WT), 76.17% $\pm$ 4.70% (GFAP-$CB_1$-KO), 57.17% $\pm$ 2.19% (GFAPhrGFP-$CB_1$-WT). Only background levels are in synaptic terminals of GFAP-$CB_1$-RS (2.19% $\pm$ 1.10%), STOP-$CB_1$ (2.36% $\pm$ .85%), $CB_1$-KO (2.14% $\pm$ 1.22%) and GFAPhrGFP-$CB_1$-KO (2.06% $\pm$ 1.52%). Data are expressed as mean $\pm$ SEM of three different animals. Data were analyzed by means of Kruskal-Wallis test and the Dunn's multiple comparison post-hoc test. ***$p < .001$; **$p < .01$; *$p < .05$. As: astrocytic processes; ter: terminal; part: immunoparticles

immunostaining, a cytoskeletal protein assembled in intermediate filament packets (Hol & Pekny, 2015), is mostly restricted to the main branches of the astrocyte. However, hrGFP is a diffusible protein extending into the delicate astrocytic processes that normally lack GFAP (Nolte et al., 2001), accomplishing better detection of the astrocyte processes. Finally, maybe there epigenetic mechanisms leading to the difference between GFAPhrGFP-$CB_1$-WT and GFAP-$CB_1$-RS, as in rescue mice re-expression was induced in the adult.

The rescue of $CB_1$ receptors in mice expressing the gene exclusively in dorsal telencephalic glutamatergic neurons (Glu-$CB_1$-RS) or in forebrain GABAergic neurons (GABA-$CB_1$-RS) (de Salas-Quiroga et al., 2015; Lange et al., 2017; Remmers et al., 2017; Ruehle et al., 2013; Soria-Gómez et al., 2014) has provided interesting insights into the sufficiency of the $CB_1$ receptor in these cells for specific brain functions and behaviors. Therefore, restoration of $CB_1$ receptor expression in

astrocytes and astroglial mitochondria could represent a new approach to assess the function of the tripartite synapse. $CB_1$ receptors in astrocytes play a key role in the two-way communication between neurons and astrocytes through rising calcium in astrocytes that modulates synaptic transmission and plasticity (Araque, Castillo, Manzoni, & Tonini, 2017; Gómez-Gonzalo et al., 2015; Martin-Fernandez et al., 2017; Navarrete & Araque, 2008, 2010; Navarrete et al., 2013; Navarrete, Diez, & Araque, 2014). Astroglial $CB_1$ receptor activation regulates astrocytic D-aspartate uptake (Shivachar, 2007) and might contribute to the brain's energy supply through the control of leptin receptors expression in astrocytes (Bosier et al., 2013). Furthermore, $CB_1$ receptor expression increases in astrocytes of the sclerotic hippocampus (Meng et al., 2014) and blockade of the astroglial $CB_1$ receptors modulates the intracellular calcium signaling dampening epileptiform activity (Coiret et al., 2012). In addition, a strong decrease in $CB_1$ receptors in
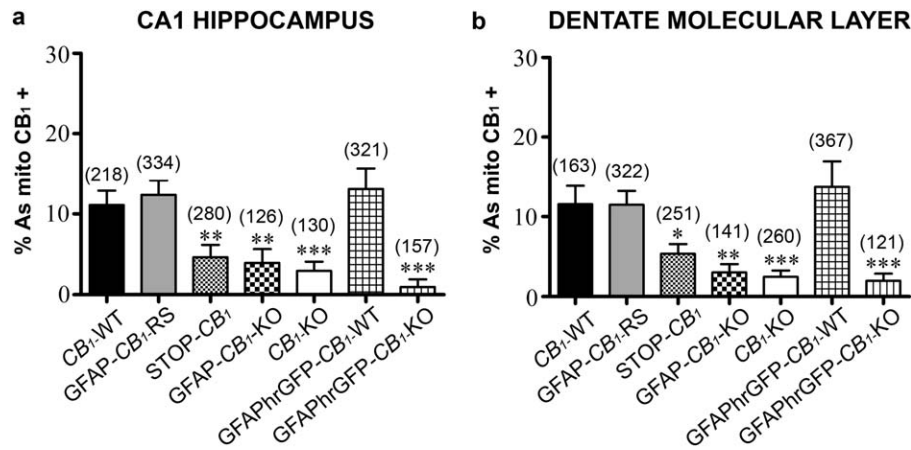
**FIGURE 7** Proportion of $CB_1$ receptor immunopositive astrocytic mitochondria in the CA1 and dentate molecular layer of wild-type and mutant mice. (a) Values of the $CB_1$ receptor immunopositive astrocytic mitochondria in GFAP-$CB_1$-RS (12.39% ± 1.81%) and GFAPhrGFP-$CB_1$-WT (13.12% ± 2.53%) are closely similar to $CB_1$-WT (11.12% ± 1.79%) in the CA1 stratum radiatum. The background in astroglial mitochondria is: STOP-$CB_1$ (4.66% ± 1.55%), GFAP-$CB_1$-KO (3.97% ± 1.71%), $CB_1$-KO (2.97% ± 1.15%) and GFAPhrGFP-$CB_1$-KO (.95% ± .95%). The number of total mitochondria examined is in parentheses on the top of each column. (b) In the dentate molecular layer, the values of $CB_1$ receptor immunopositive astrocytic mitochondria in GFAP-$CB_1$-RS (11.48% ± 1.76%) and GFAPhrGFP-$CB_1$-WT (13.74% ± 3.20%) are comparable to the $CB_1$-WT (11.56% ± 2.33%). Background in astroglial mitochondria is: STOP-$CB_1$ (5.38% ± 1.22%), GFAP-$CB_1$-KO (3.05% ± 1.04%), $CB_1$-KO (2.49% ± .80%), GFAPhrGFP-$CB_1$-KO (1.98% ± .91%). The number of total mitochondria examined is in parentheses on the top of each column. Data are expressed as mean ± SEM of three different animals. Data were analyzed by means of Kruskal-Wallis test and the Dunn's multiple comparison post-hoc test. ***$p < .001$; **$p < .01$; *$p < .05$. As: astrocytic processes; mito: mitochondria

adult mouse CA1 astrocytes has been recently observed after adolescent drinking-in-the-dark ethanol intake patterns (Bonilla-Del Río et al., 2017). Taken together, the subcellular compartmentalization of the $CB_1$ receptor in astrocytes suggests the existence of specific and precise distribution of the receptor that seems to be crucial for the functional role of the $CB_1$ receptor at the tripartite synapse (Araque et al., 2014; Araque, Castillo, Manzoni, & Tonini, 2017; Belluomo et al., 2015; Han et al., 2012; Metna-Laurent & Marsicano, 2015; Navarrete & Araque, 2008, 2010; Oliveira da Cruz et al., 2015; Perez-Alvarez et al., 2014).

## 4.1 | $CB_1$ receptors in astroglial mitochondria and potential functional implications

We estimated that 10%–15% of the total $CB_1$ receptor labeling in the hippocampus is localized at mitochondrial membranes (Bénard et al., 2012; Bonilla-Del Río et al., 2017; Hebert-Chatelain et al., 2016), and this percentage is increased in muscle and heart (Mendizabal-Zubiaga et al., 2016). Yet, about 22% of the mitochondrial sections in axon terminals and somatodendritic domains contain $CB_1$ receptors (Hebert-Chatelain et al., 2014a,b). In the present study, 11%–13% of the astrocytic mitochondrial sections were $CB_1$ receptor immunopositive,
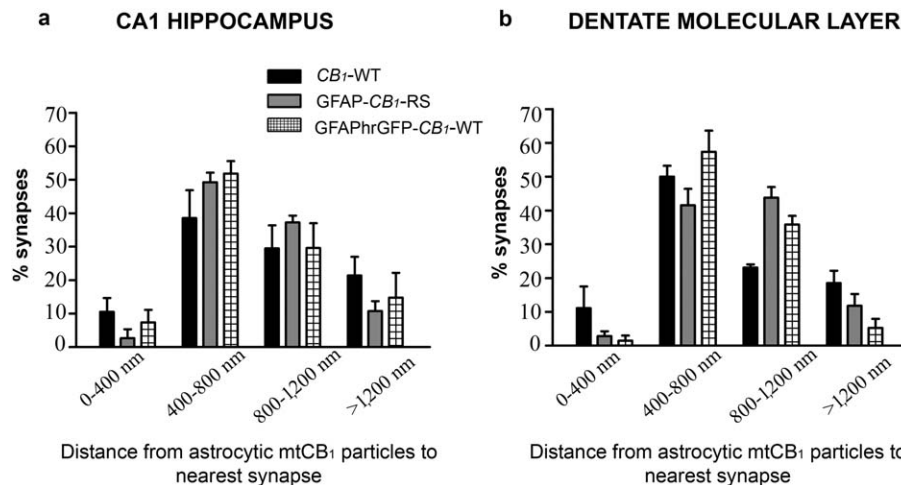


**FIGURE 8** Distance from the mitochondrial $CB_1$ receptor particles in astrocytes to the synapses in the hippocampus. The distance between the $CB_1$ receptor particles on mitocondrial membranes in astrocytic processes and the midpoint of the nearest synapse surrounded by them was assessed in the CA1 (a) and dentate molecular layer (b) of $CB_1$-WT, GFAP-$CB_1$-RS and GFAPhrGFP-$CB_1$-WT (see Table 1 for values)

**TABLE 1** Proportion of synapses visualized in 400-nm-bit ranges from the CB$_1$ receptor labeling in astroglial mitochondria

| CA1 | CB$_1$-WT (1,790 µm$^2$) | GFAP-CB$_1$-RS (2,100 µm$^2$) | GFAPhrGFP-CB$_1$-WT (784 µm$^2$) |
| --- | --- | --- | --- |
| <400 nm | 10.55% ± 4.01% | 2.67% ± 2.67% | 7.41% ± 3.70% |
| 400–800 nm | 38.54% ± 8.32% | 49.28% ± 2.87% | 51.85% ± 3.70% |
| 800–1,200 nm | 29.51% ± 6.85% | 37.26% ± 2.02% | 29.63% ± 7.41% |
| >1,200 nm | 21.40% ± 5.56% | 10.79% ± 2.94% | 14.81% ± 7.41% |
| **MDG** | **CB$_1$-WT (784 µm$^2$)** | **GFAP-CB$_1$-RS (1,708 µm$^2$)** | **GFAPhrGFP-CB$_1$-WT (1,512 µm$^2$)** |
| <400 nm | 11.11% ± 6.42% | 2.82% ± 1.48% | 1.52% ± 1.52% |
| 400–800 nm | 50.0% ± 3.21% | 41.57% ± 4.81% | 57.37% ± 6.26% |
| 800–1,200 nm | 23.15% ± .93% | 43.79% ± 3.13% | 35.86% ± 2.53% |
| >1,200 nm | 18.52% ± 3.70% | 11.82% ± 3.51% | 5.25% ± 2.72% |

indicating that mtCB$_1$ receptors in astrocytes might play important functional roles. Indeed, their activation may impact functions in which astroglial CB$_1$ receptors are involved, such as metabolic activity, neuroprotection, inflammatory responses, astrocyte development and survival, synaptic transmission, plasticity or memory formation (Aguado et al., 2006; Araque et al., 2014; Araque, Castillo, Manzoni, & Tonini, 2017; Bosier et al., 2013; Han et al., 2012; Metna-Laurent & Marsicano, 2015; Navarrete & Araque, 2008, 2010; Stella, 2010).

CB$_1$ receptors in astrocytes, but not in glutamatergic or GABAergic synaptic terminals, are responsible for long-term depression of synaptic efficacy at hippocampal CA3-CA1 synapses *in vivo* and the subsequent spatial working memory impairments induced by cannabinoid administration (Han et al., 2012). Outside of the hippocampus, endocannabinoids acting on astroglial CB$_1$ receptors in the central amygdala can regulate fear responses by selectively reducing excitatory transmission through synaptic A1 adenosine receptors and increasing inhibitory transmission by synaptic A2A receptors (Martin-Fernandez et al., 2017). Over the last decade, extensive study of mitochondrial CB$_1$ receptors has begun to establish their function and how their activity can modulate behaviors. The activation of mitochondrial CB$_1$ receptors leads to a remarkable decrease in mitochondrial respiration in brain mitochondria (Bénard et al., 2012; Hebert-Chatelain et al., 2014a,b, 2016) and the cannabinoid shutdown of hippocampal mitochondrial activity produces a decrease in cellular and mitochondrial ATP, reduces mitochondrial mobility, CA3-CA1 excitatory synaptic transmission and abolishes discrimination of novel object recognition (Hebert-Chatelain et al., 2016). The potential involvement of astroglial mtCB$_1$ receptors in these effects is currently not known and future studies will address this interesting issue.

One open question is how the (endo)cannabinoids have access to the mtCB$_1$ receptors in astrocytes. With this aim in mind we took advantage of the enhanced detection of the astrocytic CB$_1$ receptors in the CA1 stratum radiatum and dentate molecular layer of GFAPhrGFP-CB$_1$-WT mice. Then, the gap between the mitochondrial CB$_1$ receptor particles and the nearest synapse was measured to understand the anatomical relationship of the receptor in the context of the functional tripartite synapse (Araque et al., 2014; Navarrete & Araque, 2008, 2010; Navarrete et al., 2013; Navarrete, Diez, & Araque,

2014). The most frequent distance of 400–800 nm spanning up to 1,200 nm suggests that the endocannabinoids generated on demand in the postsynaptic neurons would need to travel a significant distance in order to reach the CB$_1$ receptors localized on the astroglial mitochondria. However, astrocytes are able to produce endocannabinoids (Stella, 2010), contain the main enzymes for their synthesis and degradation (Suárez et al., 2010; Uchigashima et al., 2011) and brain mitochondria also contain these lipid signaling molecules (Bénard et al., 2012). Considering that endocannabinoids can signal in autocrine, paracrine or both manners (Metna-Laurent & Marsicano, 2015), it is possible that astrocytes or even astroglial mitochondria might produce "their own" endocannabinoids to specifically activate mtCB$_1$ receptors.

Altogether, activation of intracellular CB$_1$ receptors localized at mitochondria impacts cognition through the modulation of mitochondrial energy metabolism (Hebert-Chatelain et al., 2016). Whether mitochondrial CB$_1$ receptors also regulate the organelle's energy production in astrocytes and participate in high brain functions will be elucidated in future studies.

## 4.2 | Conditional CB$_1$ receptor mutants

Loss of function in mutant mice lacking CB$_1$ receptors in specific cell types allowed insights into their anatomical localization and a deeper understanding of their necessary role for several brain functions (Bénard et al., 2012; Han et al., 2012; Koch et al., 2015; Marsicano et al., 2003; Martín-García et al., 2016; Monory et al., 2006; Monory, Polack, Remus, Lutz, & Korte, 2015; Soria-Gómez et al., 2014). Conditional mutant mice lacking CB$_1$ receptors in astrocytes exhibit neither *in vivo* hippocampal long-term depression nor the impairment of spatial working memory typically observed following acute cannabinoid treatment (Han et al., 2012). The GFAP-CB$_1$-RS mouse expressing CB$_1$ receptors exclusively in astrocytes described here, together with the Glu-CB$_1$-RS rescue mouse expressing the receptor only in dorsal telencephalic glutamatergic neurons (de Salas-Quiroga et al., 2015; Lange et al., 2017; Ruehle et al., 2013; Soria-Gómez et al., 2014) and the GABA-CB$_1$-RS rescue mouse expressing the CB$_1$ receptor only in GABAergic neurons (de Salas-Quiroga et al., 2015; Lange et al., 2017) that were recently characterized anatomically (Gutiérrez-Rodríguez

et al., 2017; Remmers et al., 2017), suggest that the regulation of the $CB_1$ receptor expression in astrocytes, glutamatergic neurons and GABAergic neurons may be independent of each others. The present demonstration that the GFAP-$CB_1$-RS in the hippocampus maintains the normal $CB_1$ receptor expression and distribution in astrocytes make these mutants ideal suited for the study of the astroglial $CB_1$ receptor function, as shown for Glu-$CB_1$-RS (de Salas-Quiroga et al., 2015; Gutiérrez-Rodríguez et al., 2017; Lange et al., 2017; Ruehle et al., 2013; Soria-Gómez et al., 2014) and GABA-$CB_1$-RS mice (de Salas-Quiroga et al., 2015; Gutiérrez-Rodríguez et al., 2017; Lange et al., 2017; Remmers et al., 2017). In fact, these rescue strategies have the advantage of the restoration and visualization of existing $CB_1$ receptor levels in locations with sparse $CB_1$ receptors (as the astrocytes and astroglial mitochondria), allowing a more comprehensive functional characterization of the (endo)cannabinoid system based on the precise cellular and subcellular localization of the $CB_1$ receptor. At the same time, these strategies improve the fundamental knowledge for the development of innovative therapeutics in the struggle against brain diseases.

Altogether, our observations confirm the high specificity of the genetic $CB_1$ receptor rescue approach carried out in the astrocytes and that these mutant mice are emerging as excellent models for studying the contribution of the $CB_1$ receptors in astrocytes and astroglial mitochondria that, although scarce in expression as compared with their neuronal counterparts, are a constant feature and likely play a key role in brain function and dysfunction.

## CONFLICT OF INTEREST STATEMENT

The authors declare that the research was conducted in the absence of any commercial or financial relationships that could be construed as a potential conflict of interest.

## ORCID

*Pedro Grandes* http://orcid.org/0000-0003-3947-4230
*Sabine Ruehle* http://orcid.org/0000-0003-0430-2367

## REFERENCES

Aguado, T., Palazuelos, J., Monory, K., Stella, N., Cravatt, B., Lutz, B., ... Galve-Roperh, I. (2006). The endocannabinoid system promotes astroglial differentiation by acting on neural progenitor cells. *The Journal of Neuroscience*, 26(5), 1551–1561. https://doi.org/26/5/1551

Araque, A., Carmignoto, G., Haydon, P. G., Oliet, S. H., Robitaille, R., & Volterra, A. (2014). Gliotransmitters travel in time and space. *Neuron*, 81(4), 728–739. https://doi.org/10.1016/j.neuron.2014.02.007

Araque, A., Castillo, P. E., Manzoni, O. J., & Tonini, R. (2017). Synaptic functions of endocannabinoid signaling in health and disease. *Neuropharmacology*, 124, 13–24. https://doi.org/10.1016/j.neuropharm.2017.06.017

Arrabal, S., Lucena, M. A., Canduela, M. J., Ramos-Uriarte, A., Rivera, P., Serrano, A., ... Suárez, J. (2015). Pharmacological blockade of cannabinoid CB1 receptors in diet-induced obesity regulates mitochondrial dihydrolipoamide dehydrogenase in muscle. *PLoS One*, 10(12), e0145244. https://doi.org/10.1371/journal.pone.0145244

Belluomo, I., Matias, I., Pernègre, C., Marsicano, G., & Chaouloff, F. (2015). Opposite control of frontocortical 2-arachidonoylglycerol turnover rate by cannabinoid type-1 receptors located on glutamatergic neurons and on astrocytes. *Journal of Neurochemistry*, 133(1), 26–37. https://doi.org/10.1111/jnc.13044

Bénard, G., Massa, F., Puente, N., Lourenço, J., Bellocchio, L., Soria-Gómez, E., ... Marsicano, G. (2012). Mitochondrial CB1 receptors regulate neuronal energy metabolism. *Nature Neuroscience*, 15(4), 558–564. https://doi.org/10.1038/nn.3053

Bezzi, P., & Volterra, A. (2011). Astrocytes: powering memory. *Cell*, 144(5), 644–645. https://doi.org/10.1016/j.cell.2011.02.027

Bonilla-Del Río, I., Puente, N., Peñasco, S., Rico-Barrio, I., Gutiérrez-Rodríguez, A., Elezgarai, I., ... Grandes, P. (2017). Adolescent ethanol intake alters cannabinoid type-1 receptor localization in astrocytes of the adult mouse hippocampus. *Addiction Biology*, Nov 23. https://doi.org/10.1111/adb.12585 [Epub ahead of print]

Bosier, B., Bellocchio, L., Metna-Laurent, M., Soria-Gomez, E., Matias, I., Hebert-Chatelain, E., ... Marsicano, G. (2013). Astroglial CB1 cannabinoid receptors regulate leptin signaling in mouse brain astrocytes. *Molecular Metabolism*, 2(4), 393–404. https://doi.org/10.1016/j.molmet.2013.08.001

Busquets-Garcia, A., Bains, J., & Marsicano, G. (2018). CB$_1$ receptor signaling in the brain: extracting specificity from ubiquity. *Neuropsychopharmacology*, 43(1), 4–20. https://doi.org/10.1038/npp.2017.206

Chiarlone, A., Bellocchio, L., Blazquez, C., Resel, E., Soria-Gomez, E., Cannich, A., ... Guzman, M. (2014). A restricted population of CB1 cannabinoid receptors with neuroprotective activity. *Proceedings of the National Academy of Sciences of the United States of America*, 111(22), 8257–8262. https://doi.org/10.1073/pnas.1400988111

Coiret, G., Ster, J., Grewe, B., Wendling, F., Helmchen, F., Gerber, U., & Benquet, P. (2012). Neuron to astrocyte communication via cannabinoid receptors is necessary for sustained epileptiform activity in rat hippocampus. *PLoS One*, 7(5), e37320. https://doi.org/10.1371/journal.pone.0037320

De Francesco, P. N., Valdivia, S., Cabral, A., Reynaldo, M., Raingo, J., Sakata, I., ... Perelló, M. (2015). Neuroanatomical and functional characterization of CRF neurons of the amygdala using a novel transgenic mouse model. *Neuroscience*, 289, 153–165. https://doi.org/10.1016/j.neuroscience.2015.01.006

de Salas-Quiroga, A., Díaz-Alonso, J., García-Rincón, D., Remmers, F., Vega, D., Gómez-Cañas, M., ... Galve-Roperh, I. (2015). Prenatal exposure to cannabinoids evokes long-lasting functional alterations by targeting CB1 receptors on developing cortical neurons.

*Proceedings of the National Academy of Sciences, 112*(44), 13693–13698. https://doi.org/10.1073/pnas.1514962112

Detsi, A., Koufaki, M., & Calogeropoulou, T. (2002). Synthesis of (Z)-4-hydroxytamoxifen and (Z)-2-[4-[1-(p-Hydroxyphenyl)-2-phenyl]-1-butenyl]phenoxyacetic acid. *The Journal of Organic Chemistry, 67*, 9489–9491.

Gómez-Gonzalo, M., Navarrete, M., Perea, G., Covelo, A., Martín-Fernández, M., Shigemoto, R., ... Araque, A. (2015). Endocannabinoids induce lateral long-term potentiation of transmitter release by stimulation of gliotransmission. *Cerebral Cortex, 25*(10), 3699–3712. https://doi.org/10.1093/cercor/bhu231

Gutiérrez-Rodríguez, A., Puente, N., Elezgarai, I., Ruehle, S., Lutz, B., Reguero, L., ... Grandes, P. (2017). Anatomical characterization of the cannabinoid CB1 receptor in cell-type–specific mutant mouse rescue models. *Journal of Comparative Neurology, 525*(2), 302–318. https://doi.org/10.1002/cne.24066

Hadaczek, P., Forsayeth, J., Mirek, H., Munson, K., Bringas, J., Pivirotto, P., ... Bankiewicz, K. S. (2009). Transduction of nonhuman primate brain with adeno-associated virus serotype 1: vector trafficking and immune response. *Human Gene Therapy, 20*(3), 225–237. https://doi.org/10.1089/hum.2008.151

Halassa, M. M., Fellin, T., Takano, H., Dong, J. H., & Haydon, P. G. (2007). Synaptic islands defined by the territory of a single astrocyte. *The Journal of Neuroscience, 27*(24), 6473–6477. https://doi.org/27/24/6473

Han, J., Kesner, P., Metna-Laurent, M., Duan, T., Xu, L., Georges, F., ... Zhang, X. (2012). Acute cannabinoids impair working memory through astroglial CB 1 receptor modulation of hippocampal LTD. *Cell, 148*(5), 1039–1050. https://doi.org/10.1016/j.cell.2012.01.037

Hebert-Chatelain, E., Desprez, T., Serrat, R., Bellocchio, L., Soria-Gomez, E., Busquets-Garcia, A., ... Marsicano, G. (2016). A cannabinoid link between mitochondria and memory. *Nature, 539*(7630), 555–559. https://doi.org/10.1038/nature20127

Hebert-Chatelain, E., Reguero, L., Puente, N., Lutz, B., Chaouloff, F., Rossignol, R., ... Marsicano, G. (2014). Cannabinoid control of brain bioenergetics: Exploring the subcellular localization of the CB1 receptor. *Molecular Metabolism, 3*(4), 495–504. https://doi.org/10.1016/j.molmet.2014.03.007

Hebert-Chatelain, E., Reguero, L., Puente, N., Lutz, B., Chaouloff, F., Rossignol, R., ... Marsicano, G. (2014). Studying mitochondrial CB1 receptors: Yes we can. *Molecular Metabolism, 3*(4), 339. https://doi.org/10.1016/j.molmet.2014.03.008

Hirrlinger, P. G., Scheller, A., Braun, C., Hirrlinger, J., & Kirchhoff, F. (2006). Temporal control of gene recombination in astrocytes by transgenic expression of the tamoxifen-inducible DNA recombinase variant CreERT2. *Glia, 54*(1), 11–20. https://doi.org/10.1002/glia.20342

Hol, E. M., & Pekny, M. (2015). Glial fibrillary acidic protein (GFAP) and the astrocyte intermediate filament system in diseases of the central nervous system. *Current Opinion in Cell Biology, 32*, 121–130. https://doi.org/10.1016/j.ceb.2015.02.004

Katona, I., & Freund, T. F. (2012). Multiple functions of endocannabinoid signaling in the brain. *Annual Review of Neuroscience, 35*(1), 529–558. https://doi.org/10.1146/annurev-neuro-062111-150420

Kerr, N., Holmes, F. E., Hobson, S., Vanderplank, P., Leard, A., Balthasar, N., & Wynick, D. (2015). The generation of knock-in mice expressing fluorescently tagged galanin receptors 1 and 2. *Molecular and Cellular Neuroscience, 68*, 258–271. https://doi.org/10.1016/j.mcn.2015.08.006

Koch, M., Varela, L., Kim, J. G., Kim, J. D., Hernández-Nuño, F., Simonds, S. E., ... Horvath, T. L. (2015). Hypothalamic POMC neurons promote cannabinoid-induced feeding. *Nature, 519*(7541), 45–50. https://doi.org/10.1038/nature14260

Kovács, A., Bordás, C., Bíró, T., Hegyi, Z., Antal, M., Szücs, P., & Pál, B. (2017). Direct presynaptic and indirect astrocyte-mediated mechanisms both contribute to endocannabinoid signaling in the pedunculopontine nucleus of mice. *Brain Structure and Function, 222*(1), 247–266. https://doi.org/10.1007/s00429-016-1214-0

Lange, M. D., Daldrup, T., Remmers, F., Szkudlarek, H. J., Lesting, J., Guggenhuber, S., ... Pape, H. C. (2017). Cannabinoid CB1 receptors in distinct circuits of the extended amygdala determine fear responsiveness to unpredictable threat. *Molecular Psychiatry, 22*(10), 1422–1430. https://doi.org/10.1038/mp.2016.156

Lu, H. C., & Mackie, K. (2016). An introduction to the endogenous cannabinoid system. *Biological Psychiatry, 79*(7), 516–525. https://doi.org/10.1016/j.biopsych.2015.07.028

Lutz, B., Marsicano, G., Maldonado, R., & Hillard, C. J. (2015). The endocannabinoid system in guarding against fear, anxiety and stress. *Nature Reviews. Neuroscience, 16*(12), 705–718. https://doi.org/10.1038/nrn4036

Magistretti, P. J., & Allaman, I. (2015). A cellular perspective on brain energy metabolism and functional imaging. *Neuron, 86*(4), 883–901. https://doi.org/10.1016/j.neuron.2015.03.035

Marsicano, G., Goodenough, S., Monory, K., Hermann, H., Eder, M., Cannich, A., ... Lutz, B. (2003). CB1 cannabinoid receptors and on-demand defense against excitotoxicity. *Science, 302*(5642), 84–88. https://doi.org/10.1126/science.1088208

Marsicano, G., & Lutz, B. (1999). Expression of the cannabinoid receptor CB1 in distinct neuronal subpopulations in the adult mouse forebrain. *European Journal of Neuroscience, 11*, 4213–4225.

Marsicano, G., Wotjak, C. T., Azad, S. C., Bisogno, T., Rammes, G., Cascio, M. G., ... Lutz, B. (2002). The endogenous cannabinoid system controls extinction of aversive memories. *Nature, 418*(6897), 530–534. https://doi.org/10.1038/nature00839

Martin-Fernandez, M., Jamison, S., Robin, L. M., Zhao, Z., Martin, E. D., Aguilar, J., ... Araque, A. (2017). Synapse-specific astrocyte gating of amygdala-related behavior. *Nature Neuroscience, 20*(11), 1540–1548. https://doi.org/10.1038/nn.4649

Martín-García, E., Bourgoin, L., Cathala, A., Kasanetz, F., Mondesir, M., Gutiérrez-Rodriguez, A., ... Deroche-Gamonet, V. (2016). Differential control of cocaine self-administration by GABAergic and glutamatergic CB1 cannabinoid receptors. *Neuropsychopharmacology, 41*(9), 2192–2205. https://doi.org/10.1038/npp.2015.351

Mendizabal-Zubiaga, J., Melser, S., Bénard, G., Ramos, A., Reguero, L., Arrabal, S., ... Grandes, P. (2016). Cannabinoid CB1 receptors are localized in striated muscle mitochondria and regulate mitochondrial respiration. *Frontiers in Physiology, 7*, 476. https://doi.org/10.3389/fphys.2016.00476

Meng, X. D., Wei, D., Li, J., Kang, J. J., Wu, C., Ma, L., ... Jiang, W. (2014). Astrocytic expression of cannabinoid type 1 receptor in rat and human sclerotic hippocampi. *International Journal of Clinical and Experimental Pathology, 7*, 2825–2837.

Metna-Laurent, M., & Marsicano, G. (2015). Rising stars: Modulation of brain functions by astroglial type-1 cannabinoid receptors. *Glia, 63*(3), 353–364. https://doi.org/10.1002/glia.22773

Monory, K., Massa, F., Egertová, M., Eder, M., Blaudzun, H., Westenbroek, R., ... Lutz, B. (2006). The endocannabinoid system controls key epileptogenic circuits in the hippocampus. *Neuron, 51*(4), 455–466. https://doi.org/10.1016/j.neuron.2006.07.006

Monory, K., Polack, M., Remus, A., Lutz, B., & Korte, M. (2015). Cannabinoid CB1 receptor calibrates excitatory synaptic balance in the

mouse hippocampus. *The Journal of Neuroscience*, *35*(9), 3842–3850. https://doi.org/10.1523/JNEUROSCI.3167–14.2015

Navarrete, M., & Araque, A. (2008). Endocannabinoids mediate neuron-astrocyte communication. *Neuron*, *57*(6), 883–893. https://doi.org/10.1016/j.neuron.2008.01.029

Navarrete, M., & Araque, A. (2010). Endocannabinoids potentiate synaptic transmission through stimulation of astrocytes. *Neuron*, *68*(1), 113–126. https://doi.org/10.1016/j.neuron.2010.08.043

Navarrete, M., Diez, A., & Araque, A. (2014). Astrocytes in endocannabinoid signalling. *Philosophical Transactions of the Royal Society of London.Series B, Biological Sciences*, *369*(1654), 20130599. https://doi.org/10.1098/rstb.2013.0599

Navarrete, M., Perea, G., Maglio, L., Pastor, J., García de Sola, R., & Araque, A. (2013). Astrocyte calcium signal and gliotransmission in human brain tissue. *Cerebral Cortex*, *23*(5), 1240–1246. https://doi.org/10.1093/cercor/bhs122

Navarro-Galve, B., Villa, A., Bueno, C., Thompson, L., Johansen, J., & Martínez-Serrano, A. (2005). Gene marking of human neural stem/precursor cells using green fluorescent proteins. *The Journal of Gene Medicine*, *7*(1), 18–29. https://doi.org/10.1002/jgm.639

Nolte, C., Matyash, M., Pivneva, T., Schipke, C. G., Ohlemeyer, C., Hanisch, U.-K., . . . Kettenmann, H. (2001). GFAP promoter-controlled EGFP-expressing transgenic mice: A tool to visualize astrocytes and astrogliosis in living brain tissue. *Glia*, *33*(1), 72–86.

Oliveira da Cruz, J. F., Robin, L. M., Drago, F., Marsicano, G., & Metna-Laurent, M. (2016). Astroglial type-1 cannabinoid receptor (CB1): a new player in the tripartite synapse. *Neuroscience*, *323*, 35–42. https://doi.org/10.1016/j.neuroscience.2015.05.002

Perez-Alvarez, A., Navarrete, M., Covelo, A., Martin, E. D., & Araque, A. (2014). Structural and functional plasticity of astrocyte processes and dendritic spine interactions. *The Journal of Neuroscience*, *34*(38), 12738–12744. https://doi.org/10.1523/JNEUROSCI.2401-14.2014

Pertwee, R. G. (2015). Endocannabinoids and their pharmacological actions. *Handbook of Experimental Pharmacology*, *231*, 1–37. https://doi.org/10.1007/978-3-319-20825-1_1

Piazza, P. V., Cota, D., & Marsicano, G. (2017). The CB1 receptor as the cornerstone of exostasis. *Neuron*, *93*(6), 1252–1274. https://doi.org/10.1016/j.neuron.2017.02.002

Piomelli, D. (2003). The molecular logic of endocannabinoid signalling. *Nature Reviews Neuroscience*, *4*(11), 873–884. https://doi.org/10.1038/nrn1247

Remmers, F., Lange, M. D., Hamann, M., Ruehle, S., Pape, H. C., & Lutz, B. (2017). Addressing sufficiency of the CB1 receptor for endocannabinoid-mediated functions through conditional genetic rescue in forebrain GABAergic neurons. *Brain Structure and Function*, *222*(8), 3431–3452. https://doi.org/10.1007/s00429-017-1411–5

Rodriguez, J. J., Mackie, K., & Pickel, V. M. (2001). Ultrastructural localization of the CB1 cannabinoid receptor in mu-opioid receptor patches of the rat caudate putamen nucleus. *The Journal of Neuroscience*, *21*, 823–833. https://doi.org/21/3/823

Ruehle, S., Remmers, F., Romo-Parra, H., Massa, F., Wickert, M., Wortge, S., . . . Lutz, B. (2013). Cannabinoid CB1 receptor in dorsal telencephalic glutamatergic neurons: Distinctive sufficiency for hippocampus-dependent and amygdala-dependent synaptic and behavioral functions. *The Journal of Neuroscience*, *33*(25), 10264–10277. https://doi.org/10.1523/JNEUROSCI.4171–12.2013

Shivachar, A. C. (2007). Cannabinoids inhibit sodium-dependent, high-affinity excitatory amino acid transport in cultured rat cortical astrocytes. *Biochemical Pharmacology*, *73*(12), 2004–2011. https://doi.org/10.1016/j.bcp.2007.03.018

Soria-Gómez, E., Bellocchio, L., Reguero, L., Lepousez, G., Martin, C., Bendahmane, M., . . . Marsicano, G. (2014). The endocannabinoid system controls food intake via olfactory processes. *Nature Neuroscience*, *17*(3), 407–415. https://doi.org/10.1038/nn.3647

Steindel, F., Lerner, R., Häring, M., Ruehle, S., Marsicano, G., Lutz, B., & Monory, K. (2013). Neuron-type specific cannabinoid-mediated G protein signalling in mouse hippocampus. *Journal of Neurochemistry*, *124*(6), 795–807. https://doi.org/10.1111/jnc.12137

Stella, N. (2010). Cannabinoid and cannabinoid-like receptors in microglia, astrocytes, and astrocytomas. *Glia*, *58*(9), 1017–1030. https://doi.org/10.1002/glia.20983

Suárez, J., Romero-Zerbo, S. Y., Rivera, P., Bermúdez-Silva, F. J., Pérez, J., De Fonseca, F. R., & Fernández-Llebrez, P. (2010). Endocannabinoid system in the adult rat circumventricular areas: An immunohistochemical study. *The Journal of Comparative Neurology*, *518*(15), 3065–3085. https://doi.org/10.1002/cne.22382

Uchigashima, M., Yamazaki, M., Yamasaki, M., Tanimura, A., Sakimura, K., Kano, M., & Watanabe, M. (2011). Molecular and morphological configuration for 2-arachidonoylglycerol-mediated retrograde signaling at mossy cell-granule cell synapses in the dentate gyrus. *The Journal of Neuroscience*, *31*(21), 7700–7714. https://doi.org/10.1523/JNEUROSCI.5665-10.2011

Volterra, A., & Meldolesi, J. (2005). Astrocytes, from brain glue to communication elements: The revolution continues. *Nature Reviews Neuroscience*, *6*(8), 626–640. https://doi.org/10.1038/nrn1722

von Jonquieres, G., Mersmann, N., Klugmann, C. B., Harasta, A. E., Lutz, B., Teahan, O., . . . Klugmann, M. (2013). Glial promoter selectivity following AAV-delivery to the immature brain. *PloS One*, *8*(6), e65646. https://doi.org/10.1371/journal.pone.0065646

Ward, W. W., & Cormier, M. J. (1979). An energy transfer protein in coelenterate bioluminescence. Characterization of the Renilla green-fluorescent protein. *The Journal of Biological Chemistry*, *254*, 781–788.

Yu, D. D., & Forman, B. M. (2003). Simple and efficient production of (Z)-4-hydroxytamoxifen, a potent estrogen receptor modulator. *The Journal of Organic Chemistry*, *68*(24), 9489–9491. https://doi.org/10.1021/jo035164n